

Fabry–Pérot-type enhancement in plasmonic visible nanosource

Marianne Consonni, Jérôme Hazart, and Gilles Lérondel

Citation: *Appl. Phys. Lett.* **94**, 051105 (2009); doi: 10.1063/1.3039075

View online: <http://dx.doi.org/10.1063/1.3039075>

View Table of Contents: <http://apl.aip.org/resource/1/APPLAB/v94/i5>

Published by the [American Institute of Physics](#).

Related Articles

A two-dimensional nanopatterned thin metallic transparent conductor with high transparency from the ultraviolet to the infrared

Appl. Phys. Lett. **101**, 181112 (2012)

Experimental investigation of photonic band gap influence on enhancement of Raman-scattering in metal-dielectric colloidal crystals

J. Appl. Phys. **112**, 084303 (2012)

Composition, nanostructure, and optical properties of silver and silver-copper lusters

J. Appl. Phys. **112**, 054307 (2012)

Influence of alloy inhomogeneities on the determination by Raman scattering of composition and strain in Si_{1-x}Gex/Si(001) layers

J. Appl. Phys. **112**, 023512 (2012)

Plasmon coupling in circular-hole dimers: From separation- to touching-coupling regimes

J. Appl. Phys. **112**, 013113 (2012)

Additional information on *Appl. Phys. Lett.*

Journal Homepage: <http://apl.aip.org/>

Journal Information: http://apl.aip.org/about/about_the_journal

Top downloads: http://apl.aip.org/features/most_downloaded

Information for Authors: <http://apl.aip.org/authors>

ADVERTISEMENT



Goodfellow
metals • ceramics • polymers • composites
70,000 products
450 different materials
small quantities fast

www.goodfellowusa.com

Fabry–Pérot-type enhancement in plasmonic visible nanosource

Marianne Consonni,^{1,2,a)} Jérôme Hazart,¹ and Gilles Lérondel^{2,a)}

¹CEA-LETI, MINATEC, 17 rue des Martyrs, 38054 Grenoble Cedex 9, France

²Laboratoire de Nanotechnologie et d'Instrumentation Optique, Institut Charles Delaunay, CNRS FRE 2848, Université de Technologie de Troyes, 12 rue Marie Curie, BP 2060, 10010 Troyes Cedex, France

(Received 11 August 2008; accepted 9 November 2008; published online 3 February 2009)

Starting from thin film planar technology, we designed and fabricated a visible optical source that produces a localized bright spot with nanometric dimensions. The structure consists of exciting surface plasmons through the illumination of a subwavelength hole in a silver film and in confining them at the vicinity of the aperture by surrounding the hole of Bragg mirrors resonant with the plasmons generated. Both finite element method computations and experimental results evidence the performances of this device that could find applications, for example, in nanolithography or optical data storage. © 2009 American Institute of Physics. [DOI: 10.1063/1.3039075]

The ability to generate an optical nanosource is of great importance in the area such as nanolithography or optical data storage. The extraordinary optical transmission through subwavelength apertures associated with the excitation of surface plasmons by periodic corrugations has been shown to be a very efficient way to achieve a directional light beam.^{1–5} Indeed, it has been evidenced that the addition of a corrugation at the aperture input considerably enhances the structure transmission,^{1–4} while the insertion of a corrugation at the aperture exit leads to a lensing effect.^{1,5} However, the size of the corresponding spots mainly belongs to the micrometric range.

In this letter, we focus on the design and the experimental realization of an optical source that produces a light spot of nanometric dimensions. The principle of the system is schematized in Fig. 1. It consists of exciting surface plasmons through the illumination of a subwavelength hole in a silver film and in confining them at the vicinity of the aperture by surrounding the hole of Bragg mirrors resonant at the generated plasmon wavelength.

From a physical point of view, this structure combines several mechanisms. First, the illumination of the subwavelength hole in the silver film generates a localized surface plasmon at its edges. Then, this plasmon has been found to efficiently couple to an antisymmetric bound plasmon mode of the metallic film⁶ and thus propagates along the surface. In order to confine this delocalized surface plasmon at the vicinity of the hole and increase the field intensity at the exit, we have added plasmonic Bragg mirrors around the aperture. These mirrors consist of concentric metallic gratings with a pitch a of $\lambda_{sp}/2$, where λ_{sp} is the wavelength of the reflected surface plasmons. Indeed, previous works⁷ have shown that this pitch corresponds to the maximum of reflectivity for these structures. Finally, these gratings also form a plasmonic microcavity around the hole, so to say a Fabry–Pérot-type resonator. In order to obtain constructive plasmon interferences in the cavity and improve the system efficiency, we chose the inner diameter (edge to edge) D of the first ring of the gratings to match the expected resonance of the cavity.

Recent works⁸ indicate that this corresponds to a width D multiple of $\lambda_{sp}/2$.

The device fabricated here was made to work at an illumination wavelength of 532 nm. It was realized on a glass substrate covered with a PMMA layer. In order to determine the gratings characteristics, a first design without corrugations or hole was considered consisting in a stack of glass ($n=1.48$, thickness 3λ), PMMA ($n=1.49$, thickness 150 nm), silver ($n=0.055+3.43i$, thickness 50 nm), and air ($n=1$, thickness 3λ). By means of Rigorous Coupled Wave Analysis⁹ we found the wavelength λ_{sp} of the less attenuated supported plasmon eigenmode of the stack, $\lambda_{sp}=320$ nm, and thus we chose $a=160$ nm and $D=320$ nm. Finally, the depth of the grating h was initially set to 50 nm and the hole diameter was fixed to 30 nm. In order to limit the computation time, we also restricted the number of periods for the gratings to seven, the number from which we observed (computations not shown) that the intensity of the generated spot saturates.

To improve this basic design, which in fact does not take into account the influence of the nanostructures on the plasmon eigenmode wavelength, we combined two-dimensional (2D) finite element method (FEM) computations performed with matched boundary conditions with a MATLAB optimization loop. For each calculation step, the spot characteristics (intensity and dimensions) are first extracted from the field map of the structure provided by the FEM computations. Then, the structure geometry (silver thickness, pitch, depth, and position of the Bragg gratings) is slightly modified in order to increase the resolution (decrease the size) and the

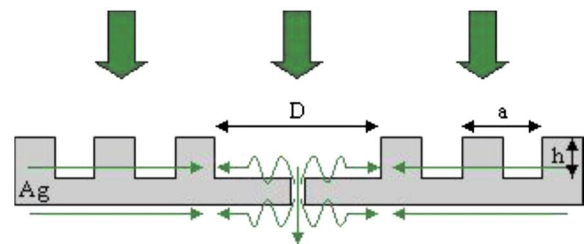


FIG. 1. (Color online) Scheme of the Fabry–Pérot-type plasmonic nanosource (cross section). A far-field illuminated subwavelength hole in a silver film generates surface plasmons, which are confined at the vicinity of the aperture by the Bragg mirrors surrounding the hole.

^{a)}Authors to whom correspondence should be addressed. Electronic addresses: marianne.consonni@cea.fr and gilles.lerondel@utt.fr.

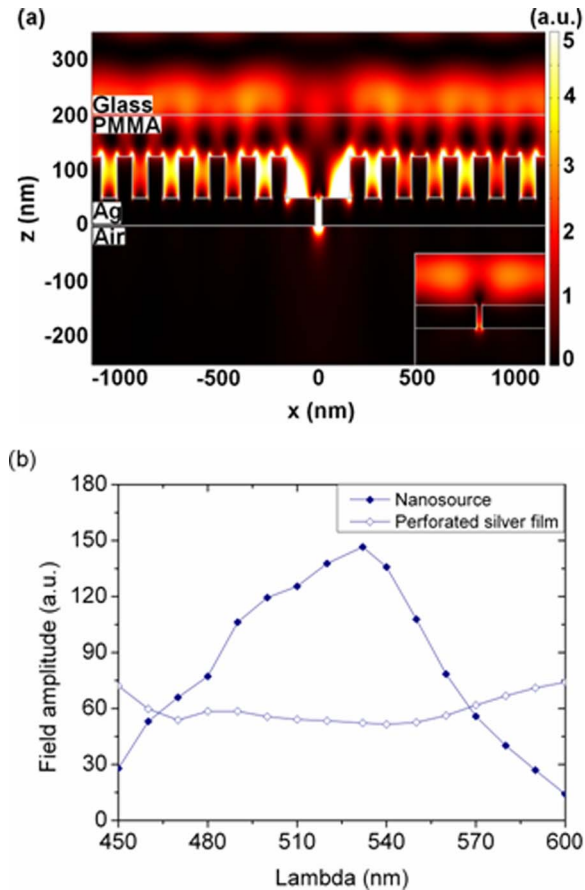


FIG. 2. (Color online) Characteristics of the nanosource after optimization. It is composed of a 50 nm thick silver film perforated with a 30 nm hole and surrounded by Bragg gratings ($a=150$ nm, $h=75$ nm, and $D=305$ nm). (a) 2D map of the field intensity in the nanosource. The field generated by the structure without gratings is also shown in the inset. Both computations were done with a FEM with a 532 nm TM polarized plane wave coming from the glass side. (b) Field amplitude taken at 100 nm from the hole exit as a function of the incident wavelength. For comparison, the results obtained for the structure without gratings are also given.

contrast of the light spot. Then, FEM computations are started again taking into account the new geometry and so forth.

The structure resulting from this optimization loop is finally composed of a 50 nm thick silver film perforated with a 30 nm hole and surrounded by Bragg gratings of 150 nm pitch and 75 nm depth. The width of the central cavity is 305 nm, which is about twice as much as the grating pitch and should be close to the effective wavelength of the plasmons excited in the complete structure. The result of the illumination of this system at normal incidence with a TM (perpendicular to the grating axis) polarized plane wave at 532 nm is presented in Fig. 2(a). This 2D map of the field intensity (i.e., EE^*) evidences a 70 nm wide hot spot localized at the vicinity of the subwavelength hole leading to a directional light beam. To verify the resonant nature of the structure, we also calculated the field amplitude generated at 100 nm from the exit of the hole as a function of the wavelength [graph given in Fig. 2(b)] for structures with (full circles) and without (empty circles) the Bragg gratings. For the first structure, a threefold spot amplitude enhancement is obtained, as expected for the illumination wavelength of 532 nm ($\lambda_{sp} \approx 305$ nm). The increase in the spot amplitude as a function

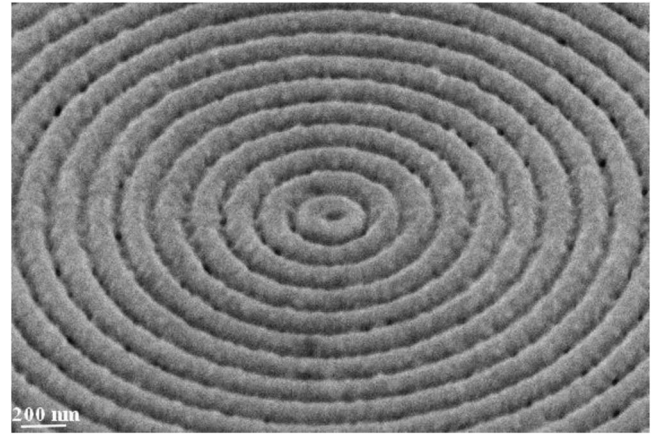


FIG. 3. Top view (scanning electron microscopy image) of the nanosource structure. The dimensions of the Bragg gratings are $a=165$ nm, $h=80$ nm, and $D=295$ nm.

of the period number of the gratings (not shown) also confirms the resonant behavior of this structure.

In order to test the performances of the proposed 2D optimized geometry on a pointlike source, we extended this structure to a three-dimensional (3D) one by radial symmetry. Indeed, considering the symmetry of the structure and an incident radial polarized excitation, all in-plane directions are equivalent. In addition, the grating mainly interacts with delocalized plasmons, that is to say, with well-defined in-plane k vectors, and thus we assume here that the 2D simulation will be sufficient to evidence the reported effect of the corrugation. However, to quantify the absolute efficiency of the proposed geometry based on a 3D nanometric aperture, 3D numerical simulation will be needed.

In order to easily “visualize” the field at the exit of the hole, we used the so-called photochemical imaging method. This method, which has been described elsewhere,¹⁰ consists of using a self-developing thin film of azo-dye polymer¹¹ whose topography, as probed by atomic force microscopy, was found to reflect the near field of metallic nano-objects. Thus, the structure parameters were changed in order to account for the presence of a 70 nm thick photosensitive azobenzene-dye polymer film of refractive index $n=1.69+0.015i$. The resulting optimized structure is composed of a Bragg grating of 165 nm of pitch and 80 nm of depth positioned on a 45 nm thick silver film and with a central cavity width of 295 nm.

The structure was fabricated in several steps. First, the mirrors were made by means of electron beam lithography in a 150 nm PMMA layer spin coated on a glass substrate and by evaporating silver on the corresponding patterns. Then, focused ion beam (FIB) was used to perforate the silver film and to obtain the final structure as shown in Fig. 3. A photoresist layer was deposited on the sample by spin coating and the system was finally exposed from the glass side using a 532 nm linearly polarized laser diode at a power density of 100 mW/cm² during 90 min. In order to approximate a radial polarized exposure, which is the most efficient incident polarization for the considered geometry, two perpendicular polarized exposures were performed. Although this approximation is theoretically inaccurate, it is valid if we consider the amount of energy received by the photosensitive film and is justified in our case by the fact that the azobenzene-dye polymer is sensitive to the field intensity.

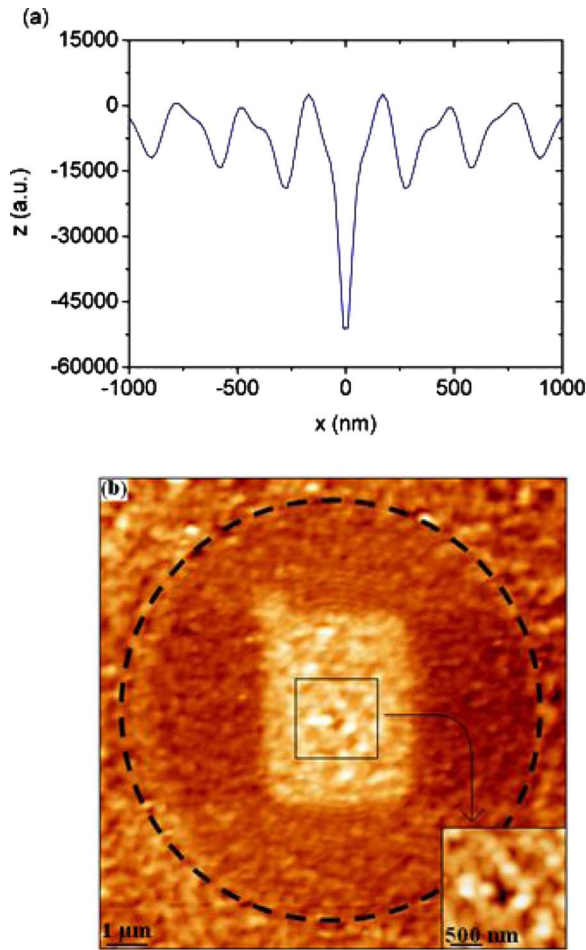


FIG. 4. (Color online) Theoretical and experimental topographies photoinduced at the surface of the photosensitive layer. (a) Expected theoretical profile provided by FEM. (b) AFM measurements of the sample surface after exposure. Bragg gratings are delimited by the dotted lines and the inset on the right is a zoom taken at the center of structure.

In order to properly analyze the experimental results, we have calculated the theoretical profile induced in the photosensitive film by the illumination of the structure. It was shown in previous works that the azobenzene-dye polymer is polarization sensitive^{10,12} and undergoes topographic modifications proportional to the following quantity:¹³

$$V = -E_x E_x^* - E_y E_y^* + E_z E_z^*, \quad (1)$$

where E_x , E_y , and E_z are, respectively, the x , y (sample plane), and z (perpendicular to sample plane) components of the electric field in the polymer. Figure 4(a) shows the corresponding profile (extracted from the 2D FEM computations of the structure) calculated at the top of the resist layer.

A deep hollow located at the vertical of the subwavelength hole in the silver film is clearly evidenced.

The atomic force microscopy (AFM) image of the sample surface after exposure is shown in Fig. 4(b). It first exhibits a rectangular swelling at the center of the structure which we believe is due to the electron beam exposure of the PMMA layer during the FIB process (a dual beam system was used here). More interestingly, it reveals the presence of a hole roughly located at the center of the system. Although slightly larger than expected [cf. the theoretical profile in Fig. 4(a)], probably because of the structure imperfection, this photoinduced feature clearly evidences the ability of the structure to generate a visible hot spot with dimensions in the nanometric range.

In conclusion, we have shown both numerically and experimentally that the association of a subwavelength hole with resonant plasmonic Bragg mirrors was efficient to generate a nanometric localized hot spot. Most direct applications of such optical nanosources lie in low cost and high resolution optical lithography or data storage.

The authors are grateful to Sergei Kostcheev from the LNIO for his support during the sample fabrication and David Troadec from IEMN who was in charge of the focused ion beam process. The “Région Champagne-Ardenne” and the European Social Found are also acknowledged for their respective financial supports.

¹F. J. Garcia-Vidal, L. Martin-Moreno, H. J. Lezec, and T. W. Ebbesen, *Appl. Phys. Lett.* **83**, 4500 (2003).

²O. T. A. Janssen, H. P. Urbach, and G. W. 't Hooft, *Phys. Rev. Lett.* **99**, 043902 (2007).

³H. J. Lezec, A. Degiron, E. Devaux, R. A. Linke, L. Martin-Moreno, F. J. Garcia-Vidal, and T. W. Ebbesen, *Science* **297**, 820 (2002).

⁴A. Degiron and T. W. Ebbesen, *Opt. Express* **12**, 3694 (2004).

⁵D. Z. Lin, C. K. Chang, Y. C. Chen, D. L. Yang, M. W. Lin, J. T. Yeh, J. M. Liu, C. H. Kuan, C. S. Yeh, and C. K. Lee, *Opt. Express* **14**, 3503 (2006).

⁶T. Rindzevicius, Y. Alaverdyan, B. Sepulveda, T. Pakizeh, M. Käll, R. Hillenbrand, J. Aizpurua, and F. J. Garcia de Abajo, *J. Phys. Chem. C* **111**, 1207 (2007).

⁷J. C. Weeber, Y. Lacroute, A. Dereux, E. Devaux, T. Ebbesen, C. Girard, M. U. Gonzalez, and A. L. Baudrion, *Phys. Rev. B* **70**, 235406 (2004).

⁸J. C. Weeber, A. Bouhelier, G. Colas des Francs, L. Markey, and A. Dereux, *Nano Lett.* **7**, 1352 (2007).

⁹E. Silberstein, P. Lalanne, J. P. Hugonin, and Q. Cao, *J. Opt. Soc. Am. A* **18**, 2865 (2001).

¹⁰C. Hubert, A. Rumyantseva, G. Léron del, J. Grand, S. Kostcheev, L. Bilot, A. Vial, R. Bachelot, P. Royer, S. H. Chang, S. K. Gray, G. P. Wiederrecht, and G. C. Schatz, *Nano Lett.* **5**, 615 (2005).

¹¹S. Bian, J. M. Williams, D. Y. Kim, L. Li, S. Balasubramanian, J. Kumar, and S. Tripathy, *J. Appl. Phys.* **86**, 4498 (1999).

¹²Y. Gilbert, R. Bachelot, P. Royer, A. Bouhelier, G. P. Wiederrecht, and L. Novotny, *Opt. Lett.* **31**, 613 (2006).

¹³M. Derouard, J. Hazart, G. Léron del, R. Bachelot, P. M. Adam, and P. Royer, *Opt. Express* **15**, 4238 (2007).